TABLE OF CONTENTS (Cont.)

LIST OF FIGURES

LIST OF PLATES

LIST OF APPENDICES

I. INTRODUCTION

Between January 13, 1989 and January 20, 1989, Barringer Geoservices, Inc., conducted a high-sensitivity drape-flown aeromagnetic/very low frequency electromagnetic (VLF) survey over a portion of the Tuscarora Mountains in northern Nevada for Chevron Resources Company. The purpose of the survey was to obtain general structural, lithological, and alteration information and to outline areas of exploration interest. This report describes the acquisition, processing and interpretation of 1900 line miles of proprietary data collected within the survey area (Figure 1).

II. DATA ACQUISITION

The contractor selected to fly the survey was Airmag Surveys, Inc., of Philadelphia, Pennsylvania. The aircraft used was a twin-engine Cessna 320, equipped with a tail stinger mounted Scintrex cesium vapor magnetometer and a nose stinger mounted Herz Totem-2A VLF receiver. The sensitivity of the magnetometer and VLF receiver were 0.01 nT and 1.8 mV respectively. Both data types were sampled every 0.25 second which resulted in an average along line sampling distance of approximately 75 feet. The data were recorded digitally and in analog form.

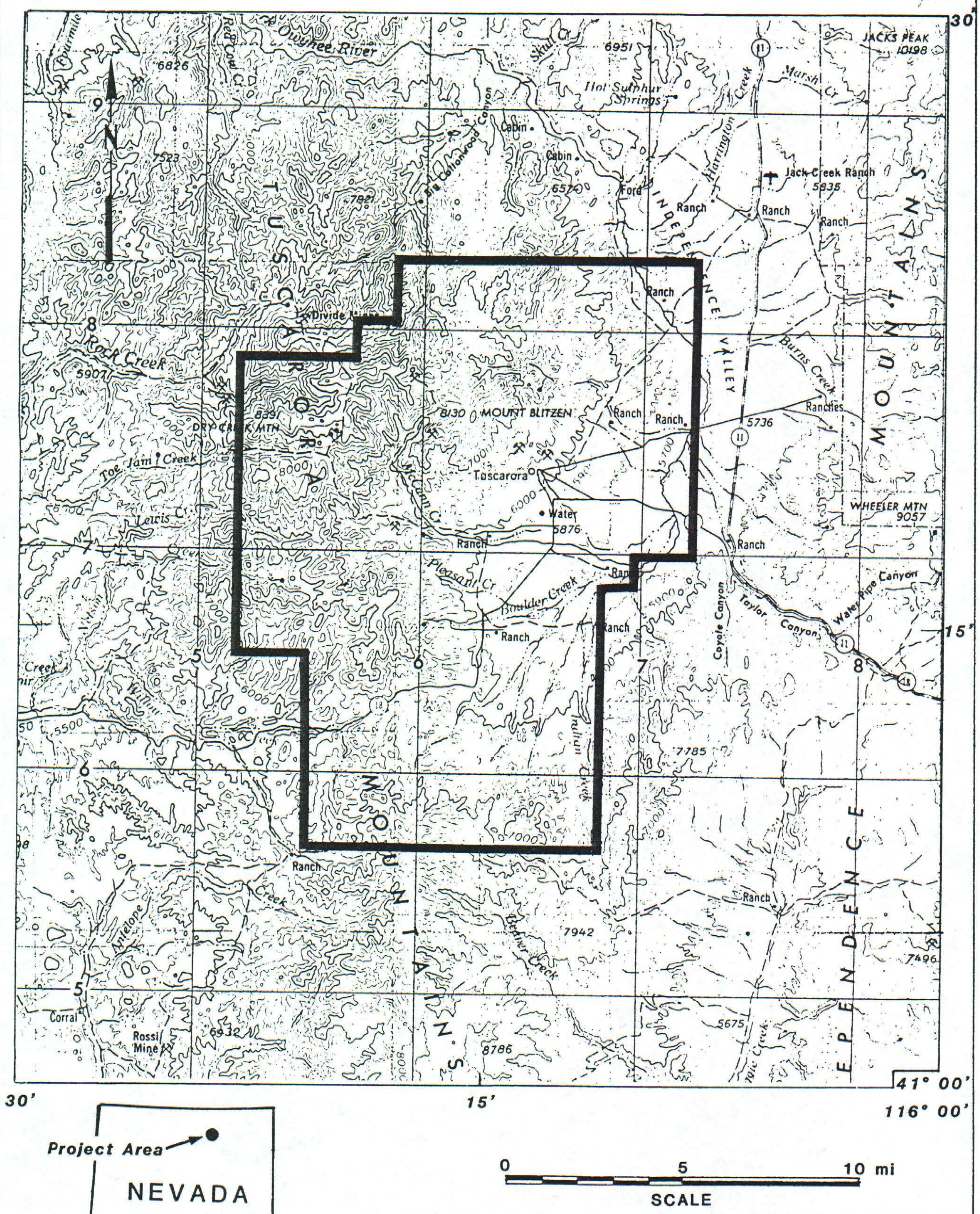

LOCATION MAP

Tuscarora Mountains, Nevada

BARRINGER RESOURCES

Figure 1

The survey was flown at a mean terrain clearance of 400 feet. Altitudes were measured with both barometric and radar altimeters and all navigation was done visually from 7 1/2 minute topographic and orthophoto quadrangles.

During flights, the earth's external, diurnal magnetic field was constantly monitored at a base station located in Winnemucca which consisted of a second cesium vapor magnetometer. Two complete days of acquired data were rejected because of severe magnetic storms, and weather conditions restricted flying on several days.

Set out below are the principal survey parameters:

Traverse-line direction:	N-S
Tie-line direction:	E-W
Traverse-line spacing:	1/8 mile
Tie-line spacing:	1/2 mile
Nominal ground clearance:	400 feet
VLF Line (Cutler, MA) Frequency	24.0 KHz
VLF Ortho (Jim Creek, WA) Frequency	24.8 KHz

Appendix A contains information for each flight line.

III. DATA COMPILATION AND PROCESSING

During the course of the survey, flight tapes, base station tapes, film strips, and analog records were dispatched to Airmag's office in Philadelphia for flight-path recovery. Ground control points on the film strip were identified and located on 7 1/2 minute topographic and orthophoto quadrangles. Manuscripts and tapes containing the picked fiducials were then shipped to Barringer's Denver facilities where they were received on February 6, 1989. The fiducials were merged with the recorded digital flight data. "Speed checks" were carried out on the data and a flight-path recovery map (Plate 1) was plotted at a scale of 1:48,000 to verify the positional accuracy of picked fiducials.

The digital data were then loaded into Barringer's geophysical data base stored on a Masscomp MC-5500 mainframe computer.

A. AEROMAGNETIC DATA

The raw aeromagnetic data were first analyzed for possible spikes, spurious noise and data steps related to the acquisition system. This was achieved by calculating the 4th difference of the data and statistically removing the identified noise, following procedures similar to those outlined by Hood, and others (1979).

The 4th difference centered on the ith data element, d_i is given by:

$$4\text{th Diff} = d_{(i+2)} - 4d_{(i+1)} + 6d_{(i)} - 4d_{(i-1)} + d_{(i-2)}$$

The standard deviation of the 4th difference is a measure of the noise envelope of the raw data. For the Tuscarora data set, the mean of the standard deviations for each line was approximately 0.25 nT.

In general, few significant spikes were detected. Most anomalous 4th difference results occurred over severe magnetic gradients associated with volcanics and igneous rocks of the area.

Following the preliminary editing, the earth's normal field, which is represented by the International Geomagnetic Reference Field (IGRF), was removed from the total intensity data set. This was achieved by fitting a second order, least-squares polynomial surface to a 2.5 minute latitude/longitude grid of IGRF approximations covering the survey area. The approximations were calculated at the mean barometric altitude of the survey using the IGRF85A magnetic model updated to January 1989. For each data point on a line, a predicted IGRF value was calculated using the polynomial. This predicted value was then subtracted from the measured total field for that data point.

Next, the remaining total intensity data were leveled and adjusted. This was done in three stages. In the first stage, the position of each traverse/tie-line intersection was located and the mistie between the magnetic values on the respective tie-line and traverse-line calculated.

In the second stage, the mean and standard deviation of the misties were calculated iteratively for each line, beginning with the tie-lines. The iterative process consisted of the initial calculation of simple statistics, followed by the calculation of a second set of statistics, using only those misties occurring within two standard deviations of the original mean. The procedure was then repeated for the traverse-lines. The mistie mean (level shift) for each line was stored for later use. Tie-line/ traverse-line iterations continued until the change in cumulative level shift became insignificant, at which point the cumulative level shifts were removed from the flight line data, resulting in a systematically leveled data set.

The third stage of the leveling/adjustment procedure was to apply "random" adjustments to the data over sections of lines where the systematic, or D.C., leveling was insufficient to adequately correct for the misties. This was achieved by fitting a least squares polynomial of an order dependent upon the number of misties to the remaining misties on each line (Yarger and others, 1978). In this way, small sections of lines were adjusted along linear trends, according to the general reliability of any given line.

Finally, the leveled and adjusted total intensity data were gridded on a 100 meter (approximately 330 feet) grid using a minimum curvature gridding routine. This grid interval is about half of the flight line spacing of 1/8 mile. The gridded data were then contoured at a scale of 1:48,000 using a 10 nT contour interval.

B. VLF DATA

Simple statistics (min, max, mean, standard deviation) were calculated for each of the two total field VLF channels. The statistics were used to calculate mean-subtracted (residual) VLF channels and standardized (normalized) VLF channels. The residual and normalized processing techniques were used to correct for zero-level and signal strength variations respectively. Each type of variation occurred commonly throughout the data acquisition period.

The normalizing technique used consisted of two steps. First, for each value on a given line, the mean for the line was subtracted from the value. Next, the residual was divided by the standard deviation for the line, leaving the resultant as a standardized value. For plotting, the standardized values were transformed back into millivolt units by first, multiplying by the mean standard deviation for the survey and second, adding the mean value for the survey. This resulted in normalized data.

For each of the total field VLF channels, both the residual and normalized data were leveled and adjusted in a manner similar to that described above for the total magnetic intensity data. It should be noted that for each total field VLF channel, the level and adjust process used the <u>same</u> frequency tie-line and traverse-line data. This is important because when the data were acquired, the tie-line and traverse-line data stored in a VLF channel were different frequencies.

After the leveling and adjusting process, both VLF total field channels were gridded and contoured at a scale of 1:48,000 using a 100 meter grid interval and a 10 millivolt contour interval.

IV. GEOLOGY

A. REGIONAL GEOLOGY AND TECTONICS

The northern Tuscarora Mountains are located in the northern Basin and Range physiographic province, near the southern margin of the Owyhee Plateau physiographic province. The Basin and Range is commonly described as a high desert area of largely interior drainage characterized by north-northeast-trending mountains and valleys. The Owyhee Plateau consists of a thick sequence (>3,000 feet) of Miocene volcanic rocks unconformably overlying Mezozoic and Paleozoic sediments in northern Nevada. The survey area has undergone a complex sequence of geologic and tectonic events (Evans and Theodore, 1978; Silberling and Roberts, 1962; Smith and Ketner, 1968; Ketner, 1977; and Stewart, 1980). The following is summarized from Speed (1983), and Stewart (1983), unless otherwise noted.

In late Precambrian to early Cambrian time, the area was located at the passive western margin of sialic continental North America. This edge is presently evidenced by outcrops of continental shelf facies or platform facies rocks, isotope ratios and mineralogy of Phanerozoic magmatic rocks, and by changes in gravity gradients that indicate changes in crustal thickness.

The early, regional geology is summarized in Figure 2. During the Antler orogeny in early Mississipian time, the Roberts Mountains allochthon was accreted to the this passive continental margin. The allochthon consists of an assemblage of pelagic and volcanic rocks that are early Paleozoic in age and probably of oceanic origin. The trace of the accretionary wedge, the Roberts Mountains thrust, occurs immediately east of the survey area.

The Golconda allochthon was accreted to the continental margin during Permian time. The Golconda allochthon is composed of rocks similar in composition to the Roberts Mountains allochthon except that they are of Mississippian to Permian age. The trace of this accretionary wedge occurs west of the survey region.

SILICEOUS AND VOLCANIC FACIES | CARBONATE FACIES

Western Eugeosynclinal Allochthonous Assemblage / Eastern Miogeosynclinal Autochthonous Overlap Assemblage

UPPER PALEOZOIC — GALCONDA THRUST

SYSTEM	FORMATION	SYSTEM	FORMATION
Permian (?)	Havallah	Permian (?)	Edna
		Upper Pennsylvanian	Antler Peak Limestone
Pennsylvanian	Pumpernickle		
		Lower Pennsylvanian	Battle

ANTLER OROGENY — *MAJOR UNCONFORMITY*

Western Eugeosynclinal Allochthonous Assemblage / Eastern Miogeosynclinal Autochthonous Assemblage

LOWER PALEOZOIC — ROBERTS MOUNTAINS THRUST

SYSTEM	FORMATION	Eastern Miogeosynclinal Autochthonous Assemblage
Ordovician	Valmy	
Upper Cambrian (?)	Harmony	No Known Outcrops
Lower and Middle Cambrian (?)	Scott Canyon	

SEDIMENTARY STRATIGRAPHY

BARRINGER

Figure 2

Evidence that the western margin remained passive through the Paleozoic includes the following phenomena: absence of magmatism and metamorphism within the continent, lack of pervasive crustal shortening or mountain-building within the continental crust, and deformation of obducted terrain consisting of only thin zones at the base of the allochthons.

In middle or late Triassic time, the continental margin underwent a passive to active transition. A continental magmatic arc emerged and crossed California and Nevada at approximately 38^{O}N. Rocks attributed to the magmatic arc include volcanogenic breccia, lava, and sediments, and plutonic granodiorite, quartz diorite, and quartz monzanite that range as young as 80 ma. Rocks associated with this magmatism occur nearest to the survey area in the Santa Rosa Mountains, the Osgood Mountains, and the Mahoganies. Smith and others (1971) conclude that these and other intrusives in northern Nevada form a link between the Sierra Nevada batholith and the Idaho batholith.

Regional middle Cenozoic geology and tectonics are influenced mainly by volcanic activity that started about 43 ma. The igneous activity started in the northern Basin and Range province and progressed southward along an arcuate east-west front, ending about 6 ma in southern Nevada. The east-west trend may suggest that north-south extension occured during the period possibly along ancient Precambrian structures. Volcanic rocks in the northern

Tuscarora Mountains area associated with this igneous activity include intermediate flows and silicic tuffs at 43-34 ma, silicic tuff at 34-17 ma, and basalt, rhyolite, and silicic tuff at 17-6 ma (Silberman, 1983, Figures 7-10, after Stewart and Carlson, 1976).

Late Cenozoic structures are primarily associated with Basin and Range faulting caused by extensional tectonics, as shown in Figure 3. Normal faults are generally oriented north to north-northeast, whereas the main mineral belts exemplified by the Carlin Trend and the Battle Mountain-Cortez trend follow northwest-southeast drag folds.

B. LOCAL GEOLOGY

1. Stratigraphy

The oldest sedimentary rocks, which belong to the Ordivician Valmy Formation, occur as two up-thrown fault blocks in the survey area. The largest, more contiguous outcrop underlies a portion of the northwest survey corner while the other, which is less contiguous and broken by faulting, occupies the southwest corner of the survey area. The Valmy Formation is a siliceous assemblage of chert, siltstone, quartzite, and greenstone that possibly has a volcanic origin. It is a member of the western facies Roberts Mountains allochthonous assemblage which was transported to its present location during the Antler orogeny in middle to late Paleozoic time (Roberts, 1964; Evans and Theodore, 1978; Stewart, 1980; and Willden, 1961).

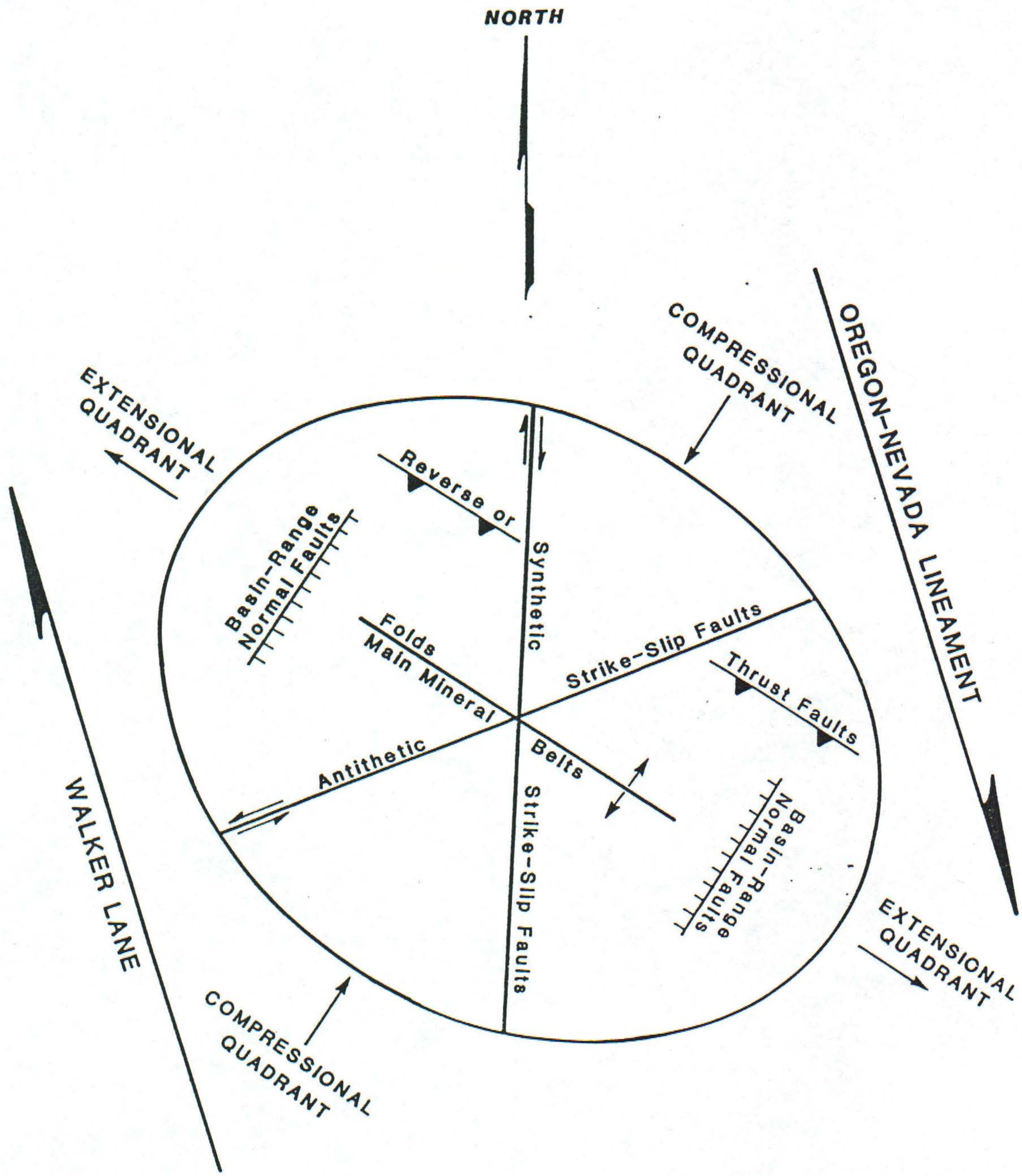

Late Cenozoic Strain Ellipsoid for Northeastern Nevada

BARRINGER

Figure 3

Small amounts of early Oligocene volcanogenic sediments occur in the extreme north-northeast survey region.

Erosion has removed extensive amounts of sedimentary and volcanic rocks. Quaternary deposits are principally sand, gravel, and silt deposited on the pediments of Independence Valley and within other stream valleys.

2. Igneous Rocks

Large amounts of early Oligocene volcanic rocks cover most of the area. These rocks consist mainly of voluminous rhyodacitic ignimgrite (welded-tuff) underlying the north-central and southeast portions of the area and andesite to basaltic andesite composition flows ringing the north-central zone of ignimbrite. Other minor outcrops of volcanics consist of small plug-domes of rhyolite and small intrusive bodies of andesite (Willden, 1961).

The granodiorite porphyry of the Mount Neva pluton is exposed over an area of approximately nine square miles in the vicinity of Dry Creek Mountain in the northwest survey corner. Age dates from the biotite in the granodiorite porphyry yield 38 ma (Coats and McKee, 1972). The texture of the granodiorite porphyry suggests that it may be genetically related to the extrusive rocks of the region (Coats and McKee, 1972).

3. Structure

The most prevalent fault trend through the northern Tuscarora Mountains is north to northeast, parallel to regional Basin and Range normal faulting. A secondary trend of northwest- trending normal faults is also present in the area. The Independence Valley to the east is a graben structure bounded in the west by normal faults trending N10°E and N40°W. Paleozoic sediments are exposed in a triangular-shaped upthrown fault block south of Dry Creek Mountain. Minor folds in the Paleozoic rocks follow the regional trend of north-northwest folding with steep axial planes.

Two north-trending curvilinear faults are mapped within the region. One is located near the extreme northwest end of the survey area. It can be traced over a length of over eight miles and separates early Oligocene flows and ignimbrite to the west from Paleozoic sedimentary rocks to the east. The other is mapped within the north-central survey region. It can be traced over a length of five miles or so and roughly divides the zone of early Oligocene ignimbrites to the west from early Oligocene andesitic flows to the east.

4. Economic Geology

The Tuscarora mining district lies within the northeastern one-third of the survey area and the Divide mine is located about three miles north of Dry Creek Mountain just north of the survey boundary. Other unnamed mineral prospects are mapped within the early Oligocene ignimbrite between the Tuscarora mining district and Dry Creek Mountain and just west of the western survey margin. The Tuscarora (Hot Sulphur) geothermal prospect lies about five miles north of the northeast survey corner.

Recorded production from the original Tuscarora mining district lists 128,165 ounces of gold and 7,138,684 ounces of silver, not including local placer gold workings. The gold and silver mineralization consists of narrow, silver-rich veins in andesitic intrusive bodies and wide, poorly defined gold-bearing fracture zones in bedded tuffaceous rocks. Mineralized vein systems trend to the north and northeast and dip steeply west. Principal ore minerals are argentite, stephanite, proustite, pyrargyrite, pyrite, enargite, arsenopyrite, bornite, chalcopyrite, sphalerite, and galena. Gangue minerals include quartz, adularia, and calcite (Nolan, 1936; Granger and others, 1957; and Roberts and others, 1971). The district exhibits a simple zoning with the silver bonanza veins concentrated in a small area north of the town of

Tuscarora and the principal gold ore body, the Dexter mine, immediately south of the town. The zonation may be due to the control on precipitation of metals from hydrothermal fluids by the respective host rocks or may be the result of supergene processes leaching soluble silver salts from the more permeable fracture system in the volcanic flows and tuffs (Granger and others, 1957).

Alteration in the gold-bearing fracture systems is much more intense than in less permeable andesitic intrusive bodies hosting the silver ore. The original minerals of the gold-bearing volcanic rocks have been replaced by quartz, adularia, and clay (dickite?) in the ore zones. Chlorite has been introduced beyond the zones of mineralization. The alteration in the silver ore zones in the andesitic intrusive rocks consists of the introduction of chlorite and calcite with slight albitization of feldspars. Buchanan, (1981 Table 1), lists the presence of propylitic, potassic, argillic, and phyllic alteration assemblages in the district.

A K-Ar age determination from adularia in a silver-rich vein from the Tuscarora district gives 38 ma, suggesting that the silver mineralization and its associated alteration is related to the emplacement of the nearby Mount Neva granodiorite porphyry pluton (McKee and Coats, 1975).

The Tuscarora geothermal prospect lies about five miles north of the northwest corner of the survey area. From Sibbett (1982),

> "The Tuscarora geothermal prospect is located at the north end of Independence Valley in northern Nevada. Thermal springs issue from Oligocene tuffaceous sediments near the center of an area of high thermal gradient. The springs are associated with a large siliceous sinter mound and are currently depositing silica and calcium carbonate .... The surface expression of the Hot Sulphur Springs thermal system is controlled by a fault zone trending N20^{o}E. Exposed argillic alteration produced by the thermal system is limited to the spring area. Quartz-sericite alteration which predates the present thermal system is present along the fault zone .... The subsurface character of the geothermal system is not known, but the geophysical and geological data are consistent with an interpretation that the reservoir is 3 to 5 km southeast of the hot springs. In this model, meteoric water circulates down along the range-front fault system and is heated at depth. The thermal waters rise along major fractures . . ."

C. DISCUSSION

The geologically mapped rocks and structures in the northern Tuscarora Mountains appear to indicate the presence of a caldera. Lipman (1984), in his comprehensive descriptive work on ash flow calderas in western North America, outlines the genesis of calderas and associated lithologic and structural characteristics.

Lithologic characteristics associated with caldera formation are summarized below (Lipman, 1984, Figure 3). The initial stage consists of precollapse volcanism. Clustered intermediate composition stratovolcanoes form over rather small plutons that are precursors (cupolas) to a large silicic magma body. The second stage involves the continuous upward migration and coalescing of plutons into a larger magma body, possibly of batholithic dimensions. This larger magma body is what feeds the voluminous ash flow eruptions. During the ash flow eruptions, concurrent collapse of the caldera occurs. After the ash flow stage and possibly owing to a reheating event, the magma body resurges upward and intrudes the ash flow sequence. These lithologic characteristics are manifested within the survey area in the northern Tuscarora Mountains in the form of intermediate composition flows, silicic ignimbrite, and granodioritic porpyhry.

General structural characteristics associated with calderas are as follows. During the first, intermediate composition volcano-building phase, uplift of the area associated with emplacement of the plutons occurs. This may lead to the initial development of arcuate zones of ring fractures that delineate the uplifted region. During the ash flow eruptions, the increase in thickness and weight of the volcanic pile coupled with decrease in pressure in the area near the top of the batholith causes collapse of the volcanics into the caldera. The area of collapse is normally the area of greatest uplift, usually the interior zone bounded by the ring fault zone. Upon resurgence, extensional graben faults may form over the crest of the dome. These structural characteristics are manifested within the survey area in the form of arcuate normal faults that nominally form the boundary zone between volcanic units.

Many authors, including Lipman (1981, 1982, and 1984); Rytuba (1981); Worthington (1981); Guilbert and Park (1986); Buchanan (1981); and Bonham (1988), have described mineralization occurrences related to caldera environments specifically and volcanic environments in general, and have formulated models for mineralization. The following is a cursory summary of some of the more common information presented by these authors.

Cogenetic mineralization is usually associated with hydrothermal systems that form in a similar spatial as well as temporal setting to caldera formation. Mineralization can occur in at least three ways; vein and/or fracture filling, disseminated deposits, and exhalite deposits. Vein filling can be associated with either or all of the above described caldera-related structures. Disseminated deposits can occur in any porous and permeable area. Porosity may be due to either rock type characteristics or structural preparation. Exhalite deposits are found near the paleosurface and may be related to fumarolic emanations directly related to volcanic activity.

Mineralization genetically unrelated to caldera formation can occur in any caldera environment. Later intrusive activity can provide the heat source to drive hydrothermal systems. Earlier structural and stratigraphic preparation could provide the permeability necessary for the formation of any of the above described three mineralization types.

V. INTERPRETATION

A. NATURE OF THE TOTAL MAGNETIC INTENSITY MAP

The total magnetic intensity map (Plate 2) reflects the distribution of magnetic material within the survey area. Magnetite (Fe_3O_4) is the most dominant magnetic mineral and rocks containing even small amounts produce characteristic magnetic signatures. Igneous rocks, especially of the mafic to ultramafic variety, produce strong signatures and anomalous gradients, whereas unaltered sedimentary rocks devoid of magnetite do not produce anomalies. Altered, or mineralized host sediments may also be magnetic, in which case pyrrhotite (FeS) may also contribute to the magnetic effect.

The total intensity of the residual magnetic field shown on Plate 2 is proportional to the magnitude of the earth's inducing field. In the survey area, the inducing field acts at an average inclination of 66°N and declination of 15.9°E. This means that each anomaly is slightly dipolar and also slightly displaced to the southeast of its source. Remanent magnetization of the source, if present, could also further distort resultant anomalies.

The form of an individual anomaly from a given source body depends upon:

1. The direction of the earth's inducing field at the location of the body.
2. The direction of remanent magnetization of the rocks forming the body.
3. The orientation of the body with respect to the earth's field.
4. The orientation of the body with respect to the aeromagnetic flight-line.
5. The geometry of the body.

All of these factors, with the possible exception of the direction of remanent magnetization of the body, are compensated by the process known as reduction-to-pole, described in a later section.

In addition to the above five points, the survey flying height determines the amplitude of individual anomalies. The lower the altitude, the greater the measured response, but also the greater the interference from volcanic material, which is often of less importance to exploration.

B. OVERVIEW OF THE TOTAL MAGNETIC INTENSITY MAP

In the Tuscarora Mountains survey area, the most magnetic rocks consist of the granodioritic porphyry of the Mount Neva pluton. These rocks are labeled as Tgd on Willden's preliminary geologic map of Humboldt County (Willden, 1961). The anomalies are predominantly positive and result from normal induced magnetization.

Other large strong magnetic anomalies occur over intermediate to rhyolitic units located in two areas within the survey. The first encompasses about 15-20 square miles in the NE corner. Rocks mapped here include andesitic flows and ignimbrite/ volcanic sediments labeled Ta, Tt, and Tts respectively (Willden, 1961). The second anomalous area occurs as a swath from the western survey margin striking toward the southeast. Both the east and west ends are about 3-5 miles wide while the center averages about two miles wide. Rocks mapped, from west to east, include intermediate flows and ignimbrite labeled as Ta and Tt respectively. The anomalies in these areas are mostly negative, representing remanent magnetization.

Strong magnetic anomalies relatively small in areal extent occur in two areas within the survey boundaries. The first occurs over andesitic flows, mapped as Ta, cropping out within the Tuscarora mining district. These anomalies cover about two square miles and are positive, reflecting normal induced magnetization. The second occurs over outcrops of ignimbrite mapped Tt in the southern portion of the survey. These anomalies cover about two square miles and contain strong positive as well as strong negative components, probably representing both normal induced magnetization and remanent magnetization respectively.

Two areas containing moderate positive anomalies occur near the northern margin of the survey. The first occurs about one mile northeast of the mapped granodioritic porphyry and the second is located about 3.5 miles east of the mapped granodioritic porphyry. Both of these anomalies occur over rocks mapped as ignimbrite (Tt), and each is about one square mile in area. Curiously, most of the ignimbrite in this area exhibits a nonmagnetic signature, perhaps owing to its predominantly felsic nature.

Other, smaller magnetic anomalies occur over rocks mapped mainly as ignimbrite containing xenoliths of andesitic rocks. Some of the anomalies occur directly over small outcrops of andesitic (Ta) rocks while others occur over ignimbrite (Tt). In the north-central portion of the survey area, rocks mapped as andesitic crop out in a variety of locations between the Mt. Neva granodioritic porphyry and the Tuscarora mining district. A few of these outcrops exhibit anomalous magnetic signatures whereas most do not.

Generally, the sedimentary rocks in the area, represented by the Valmy formation, are nonmagnetic.

C. SPECTRAL ANALYSIS

Spectral analysis is conducted in the frequency domain and may be defined as the decomposition of a signal into its harmonic constituents. Its main purpose is to isolate the dominant periodic components, which then can be correlated with the major geological units of the area (Spector and Grant, 1970; Spector, 1968; and Spector, 1975). More specifically, this means that the main geological signal(s) can be identified and subsequently separated from the higher frequency error-noise.

The power spectral density - that is the power spectrum - of the Tuscarora aeromagnetic data, is shown in Figure 4. It was produced by first removing the mean from the total magnetic intensity data and then applying the following two dimensional Hanning window:

$$W = 1/4 \left(\left(1 + \cos\left(\frac{(2\pi f x)}{L_x}\right)\right) \cdot \left(1 + \cos\left(\frac{(2\pi f y)}{L_y}\right)\right)\right)$$

The Hanning window effectively reduces the data to the zero level along the edges of the data set thereby producing a continuous data set which is not subject to Gibbs phenomenon when transformed into the frequency domain. The Hanning window has virtually no effect on the frequency content of the data.

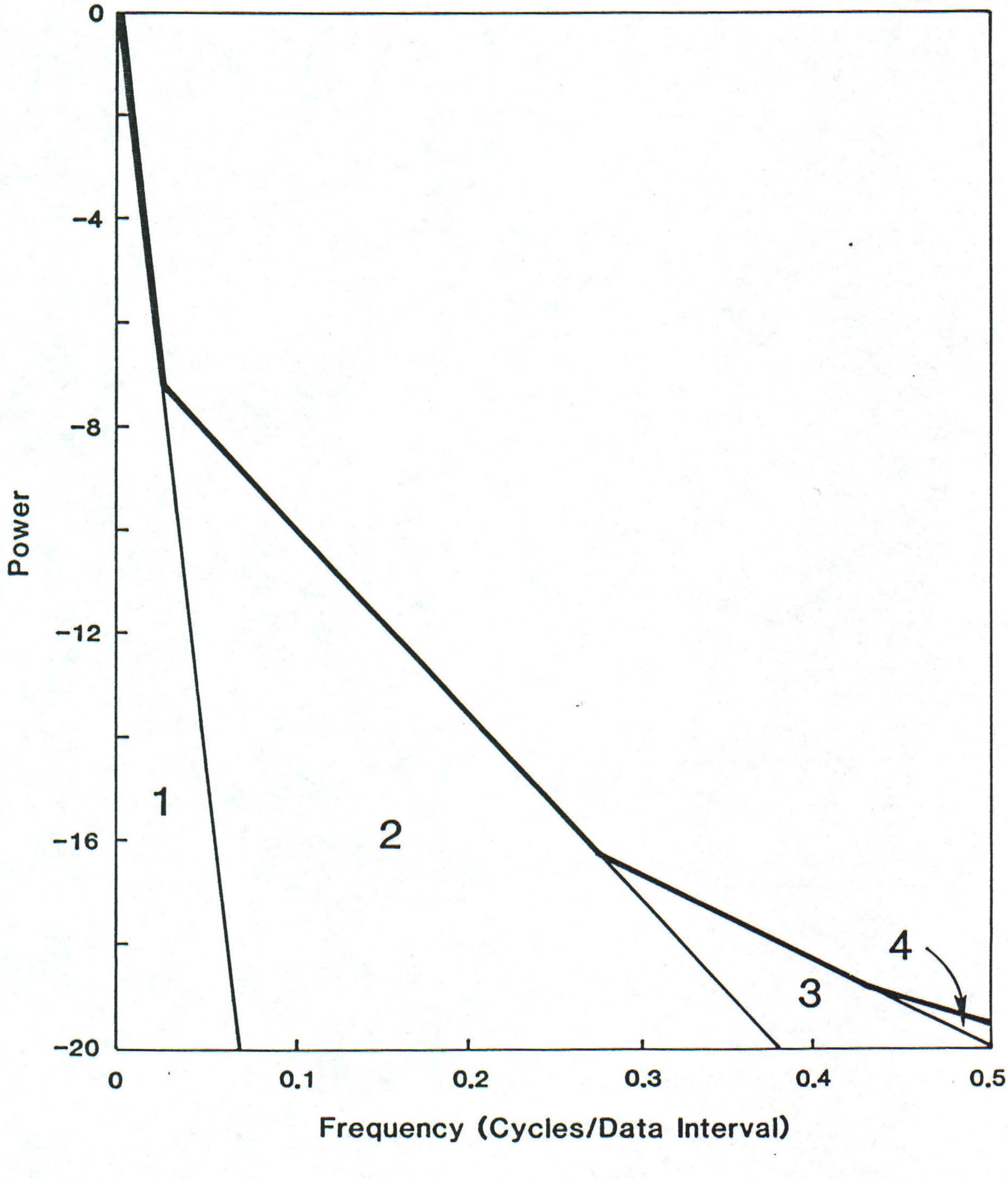

POWER SPECTRAL DENSITY
Tuscarora Mountains, Nevada

BARRINGER

Figure 4

Next, the complex spectrum coefficients of the data were calculated by use of a forward Fast Fourier Transform (FFT). The complex coefficients were reduced to the two dimensional power spectrum by taking the square of the modulus:

$$\text{Power} = [(\text{Real coefficient})^2 + (\text{Imaginary coefficient})^2]^2$$

In order to convert the two dimensional spectrum into more meaningful terms, it was next normalized, then converted to natural logarithms and finally radially averaged to produce a one dimensional spectrum. The radial frequency from the center of the spectrum is given by:

$$r = (f_x{}^2 + f_y{}^2)^{1/2}$$

where f_x and f_y are the spatial frequencies in the x and y directions respectively. The radial frequencies were than averaged into bins to produce the radial average (Spector, 1968).

The semi-logarithmic plot of the radially-averaged, normalized power spectrum shown in Figure 4 consists of logarithmic values of power and, therefore, the spectrum exhibits straight line components. These represent both the magnetic signal contributions of individual assemblages of source bodies, and also in the high frequency range, error-noise resulting from data acquisition and processing. As may be seen, there are four individual components, each of whose slope is a function of the expected value of the maximum average depth to the top of each magnetic ensemble.

Component 1 represents a magnetic assemblage with an average depth of about 7,600 feet. It is unclear what this assemblage represents except that it is probably associated with buried igneous rocks. Components 2 and 3 both represent near-surface magnetic sources, occurring between ground surface and an average depth of about 150 feet. Component 4 gives no meaningful depth and represents the Dirac comb which results from the Fast Fourier Transform.

D. POLARIZED TOTAL MAGNETIC INTENSITY MAPS

In order to minimize the dipolar distortion of the total magnetic intensity anomalies, an operation termed reduction-to-pole (polarization) was performed on the data. The polarization operation recreates the magnetic field as it would be at the earth's magnetic poles, where the inducing force is vertical.

The polarized magnetic intensity (PMI) map (Plate 3) of the area gives a good overall picture of the magnetic environment, while minimizing the distortion inherent in the total magnetic intensity data owing to the inclination and declination effects. Its main advantage is that PMI anomalies occur directly over their causative source bodies, assuming any remanent magnetization is reversed and antiparallel to the present field. As well as providing a better correlation between individual anomalies and their sources, the anomalies are also substantially better resolved than their total intensity counterparts. Generally, total intensity dipoles are reduced to single poles.

The PMI operation was carried out in the frequency domain, using the following operator, after Gunn (1975).

$$R(u,v) = \frac{(u^2 + v^2)^{1/2}}{D_1} \cdot \frac{(u^2 + v^2)^{1/2}}{D_2}$$

where D_1 is the factor for the direction of the earth's inducing field.

D_2 is the factor for the magnetization of the body, and u and v are wave numbers.

Because the PMI process enhances high frequency noise at the expense of true signal, the data were first low-pass filtered to remove the noise indicated by the spectrum, before applying the function above. The cut of frequency was 0.25 cycles/data interval, ramped to 0.375 cycles/data interval, according to the method of Cordell and Grauch (1982).

The data were then returned to the space domain as plotted on Plate 3. As may be seen, the PMI data are slightly smoother than the total magnetic intensity data. Close inspection reveals that the PMI anomalies have been shifted slightly to the north of their total magnetic intensity counterparts.

The inclination and declination used in the process was 66°N and 15.9°E respectively.

E. FIRST VERTICAL DERIVATIVE OF THE POLARIZED TOTAL MAGNETIC INTENSITY MAP

For potential field data, the first vertical derivative (FVD) is obtained by applying the following operator in the frequency domain, after Gunn (1975).

$$F(u,v) = 2\ (u^2 + v^2)^{1/2}$$

where u and v are wave numbers

In the present survey the above operator was applied to the PMI data, so that anomalies still occur over their causative source.

The FVD map (Plate 4) delineates faults and geological contacts with greater definition than the PMI map. The zero contour of the FVD map approximately defines magnetic boundaries that often correlate with faults or geological contacts. Individual magnetic features associated with granitic intrusive bodies and areas of alteration are especially well defined on the FVD map. Large areas of siliceous sedimentary rocks and ignimbrite are devoid of significant FVD anomalies. Because of the better definition of geological features on the FVD map than the PMI map, the interpretation of magnetic discontinuities and the definition of the magnetic provinces was completed primarily using the FVD map.

F. APPARENT SUSCEPTIBILITY MAP

Recent developments have shown that a combination of linear filters, known as apparent magnetic susceptibility mapping, lends itself to near-surface exploration. The apparent magnetic susceptibility map (Plate 5) gives a better picture of the compositional and lithologic features of exploration interest than any of the other maps, because regional effects have been attenuated and the data have been downward continued (Yunsheng and others, 1985). Additionally, the map units are in apparent susceptibility units which could be correlated with measurable rock properties.

In order to carry out the process, the following assumptions are made.

1. The measured magnetic field is caused by an assemblage of vertically sided infinite prisms of rectangular cross-section.

2. Magnetization is induced or antiparallel to the earth's existing field.

Both the cross-sectional size of the prism and any departure from vertical dip will affect, but not radically change, the calculated apparent susceptibilities, which should be used in a semi-quantitative manner since they have not been tied to measured susceptibilities.

As with the FVD map, large areas of the apparent magnetic susceptibility map are devoid of anomalies, especially within the large area underlain by the Valmy formation in the west and south, and ignimbrite in the northwestern half of the survey area. Significant apparent susceptibility anomalies occur over the granodiorite prophyry and some intermediate composition flows.

Also of note is that almost the entire northwest half of the survey area is of a higher susceptibility than the remainder. It is possible that the susceptibility map best outlines a buried cogenetic batholith.

G. OVERVIEW OF THE VLF EXPLORATION TECHNIQUE

Electrical prospecting methods rely on the measurement of secondary magnetic fields generated by conducting bodies in the ground when subjected to a primary electromagnetic signal. The VLF radio wave method uses radiation from the power transmitters operating for submarine navigation and communication purposes (Phillips and Richards, 1975). The range of the transmitters is considerable, and usually an overlap of signals produces a choice of frequencies in any exploration area.

The radiation from the transmitters contains both electric and magnetic components. In mineral exploration, the magnetic component is generally used since it carries the bulk of the signal energy below ground, and also offers certain advantages in field measurement. Essentially, the alternating primary magnetic signal induces an electrical current in a conductor, which gives rise to an associated secondary magnetic field.

Because of the phase difference of the alternating fields, the resultant of the primary and secondary components changes direction and makes a complete elliptical revolution during each cycle. The Totem-2A used for the present survey measures the change in the total field, as a percentage of the primary field, and also the ellipticity of the resultant field, in terms of the vertical quadrature. The two transmitting stations used were Jim Creek, Washington (24.8 KHz) and Cutler, Maine (24.0 KHz).

Airborne VLF data are used mainly for mapping of faults and conductive lithological units. However, in favorable geological areas, smaller massive sulphide conductors can be detected and alteration zones outlined.

H. VLF - TOTAL FIELD - CUTLER FREQUENCY MAP

Two maps were produced that show residual and normalized Cutler total field VLF data (Plates 6 and 7 respectively). The normalized data were interpreted because they exhibited a greater degree of continuity than the residual data. This interpretation was accomplished at the expense of a loss of some of the quantitative information present in the residual data, but after some subjective analysis, it was decided that the dividends outweighed this expense.

The Cutler VLF map can be broken into three major provinces, each of which is separated from the others by a major discontinuity.

The first province comprises the northwest portion of the survey area. Here the grain of the VLF anomalies is about N55°E and their strength or amplitude is the highest anywhere within the survey are. Rocks in the area contain the Mt. Neva granodioritic porphyry in the west and ignimbrite in the east. It is separated from the other two provinces by a major N55°E discontinuity in the south and a north-south discontinuity in the east.

The second province wholly contains the southwest half of the survey area. In this province the grain of the VLF anomalies is more ambiguous with the prevalent direction being east-west in the west, and north-south in the east. Generally, the province consists of Valmy formation rocks in the northwest and south, with andesitic flow rocks in the north, and ignimbrite in the southeast. It is bounded to the northeast by a major N50^{o}W discontinuity.

The third major VLF province comprises the remainder of the survey area, roughly containing the east-central one-third. The fabric of the VLF anomalies here is north-south. This area contains the north-south discontinuity described as the eastern terminus of the first province. This discontinuity forms a high conductivity zone over the Tuscarora mining district.

Anomalous VLF areas that warrant description are: first, the conductivity high that nearly surrounds the outcropping portion of the granodioritic porphyry, interpreted as an alteration zone; second, the conductivity low located in the center of the survey area, also interpreted as an alteration zone; and third, the large conductivity high/low anomaly located in the northeast that occurs over pediment. It is difficult to interpret but may represent some sort of moisture content/water table variation.

I. VLF - TOTAL FIELD - JIM CREEK FREQUENCY MAP

Two maps were produced that show residual and normalized Jim Creek total field VLF data (Plates 8 and 9 respectively).

The normalized data only were interpreted for reasons similar to those outlined above for the Cutler data.

The Jim Creek VLF map can also be broken into three provinces that are similar in size and shape to the provinces described in the previous section. Province boundaries remain as major discontinuities. Only anomaly amplitudes and anomaly strike directions change. Generally, the highest amplitudes are located in the southwestern province (opposite of the Cutler results) and the predominant anomaly strike direction throughout the survey area is N20^{o}W (approximately the direction toward the transmitter).

Two of the previously mentioned VLF anomalies are also present in the Jim Creek data, only at subdued levels. The VLF high surrounding the Mt. Neva granodioritic porphyry is present and the large VLF low in the center of the survey area is present, although more distorted. Both of these features have been interpreted as alteration zones.

The VLF high over the Tuscarora mining district is apparent but the link with the major north-south Cutler discontinuity is not direct.

J. INTERPRETATION MAP

The interpretation map (Plate 10) summarizes both the quantitative and qualitative details from the aeromagnetic data and the qualitative details from the VLF data. It should be used primarily as an overlay to a 1:48,000 scale geologic map and also in conjunction with the apparent susceptibility, FVD, and normalized Cutler transmitter VLF maps.

The interpretation map shows the following:

1. Four exploration areas labeled 1 through 4 covering the principal regions where ground follow-up is recommended.

2. Magnetic zones which are interpreted to be intrusive rocks.

3. The main magnetic discontinuities which represent either geological faults or strong magnetic susceptibility boundaries (geological contacts).

4. The main boundaries between magnetic provinces. Magnetic provinces are defined as areas that contain similar magnetic characteristics such as; anomaly size, anomaly amplitude, and/or apparent susceptibility.

5. The estimated depths in feet from the surface to the top of magnetic sources.

6. The main boundaries between VLF provinces. VLF provinces are defined as areas containing similar VLF signatures including anomaly size, anomaly amplitude, and direction.

7. The principal VLF anomalies or anomalous zones.

The magnetic features illustrated on the interpretation map were derived largely from the apparent susceptibility and FVD data. The VLF features were derived from the normalized Cutler transmitter total field VLF data. The estimated depths were derived by performing a 3-dimensional Euler inversion of the data using a proprietary Barringer technique. The depths were corrected for flying height using the radar altimeter data.

The four exploration areas outlined on the interpretation map are discussed below.

1. Area 1

Area 1 contains the Tuscarora mining district, and from an exploration standpoint, it merits the highest priority. The district is located along the southern end of an over four mile long previously mapped curvilinear fault. The fault may be a principal control for the existing mineralization because it could represent the eastern ring fault of the hypothesized collapsed caldera. On the interpretation map, the fault is best represented by a major VLF discontinuity. To the west of this zone, VLF anomalies and anomalous zones trend N55^{O}E, while to the east, VLF anomalies follow a more north-south grain. Rytuba (1981,p.234) introduces a model for mineralization locations and types that may be associated with a caldera environment. He explains the genesis for some of the mineralized veins associated with the Lake City caldera in southwestern Colorado in the following way:

> "Veins of Ag, Au, Pb, and Zn are distributed around the north and east part of the caldera, just outside the ring fracture zone and within the moat of the older Uncompahgre caldera.... The veins have been divided ..... into two distinct systems on the basis of age, mineralogy, and fluid composition. The older system of veins consist of quartz, barite, and base metals, and occupies concentric and radial fractures and faults on the north side of the caldera. Mineral zoning, as well as decreasing fluid inclusion filling temperatures and salinities indicate that the fluids originated from a convecting hydrothermal cell generated by the emplacement of granite porphyry during resurgence of the caldera."

Lipman (1984) reiterates the relationship between hydrothermal activity and mineralization in caldera environments and also elaborates on the fluids which are an integral part of the hydrothermal systems. In summary, low oxygen-isotope meteoric waters can enter the system and pick-up metals such as Cu and Zn that occur in the volcanic pile.

The similar age dates for veins in the Tuscarora district and the Mt. Neva granodioritic pluton (about 38 Ma) allow the above information to be applied to this area. As the pluton was being emplaced, a hydrothermal system evolved over it. Metals were concentrated in hydrothermal fluids as they circulated through the system, and in areas where boiling occurred, the metals were deposited. Buchanan (1981) introduces this type of model in a paper in which he reports the results of a study of over 60 precious metal vein deposits hosted in volcanics and Bonham (1988) further illustrates model characteristics.

The magnetic anomaly over the mining district appears to be related to the andesitic rocks and not directly to mineralization. However, the local apparent susceptibility values of about 1000 micro cgs units are more in line with the apparent susceptibilities of the intrusive rocks in the area, rather than the extensive andesites. A major magnetic discontinuity cuts the district in an approximate N10°E direction, a direction that is subparallel to the ring fault. A VLF anomaly is centered over the southernmost extent of this discontinuity. The VLF anomaly is interpreted to represent alteration and continues southward into the pediment. Other major directions of magnetic discontinuities are N60°-75°E, N40°W, and N80°W. Some of these may represent radial fractures away from the ring fault.

When studying the FVD map, one area exhibiting some magnetic characteristics that are similar to the mining district occurs in the pediment about 1.5 miles to the northeast. Here, magnetic discontinuities trend in approximately the same directions and anomaly sizes are roughly the same. The major difference is that the anomaly is negative, the opposite of that at Tuscarora. This phenomenon might be explained by alteration causing magnetite depletion in the andesitic rocks. Both the interpreted alteration and its spatial and morphological association with the mining district make this area prospective.

The middle section of Area 1 is formed by the major VLF discontinuity that subparallels the eastern mapped curvilinear fault. There are minimal numbers of readily apparent magnetic anomalies or discontinuities associated with this area, but it is included in the exploration block because of its proximity to the mapped fault.

Perhaps the most interesting area in Area 1, aside from the mining district, is the extreme north. This area contains a magnetic anomaly interpreted to indicate intrusive rocks from its relatively high (over 1000 micro cgs units) apparent susceptibility, at a depth of about 600 feet. Also, a series of parallel magnetic discontinuities striking N5^{o}-10^{o}E, some of which are adjacent to the interpreted intrusive, predominate. A VLF anomaly suggesting alteration occurs over the area immediately east of the interpreted intrusive.

It should be noted that although the volcanic rocks to the east of exploration Area 1 are not included in the block, their geophysical character is similar to that of the Tuscarora mining district. If further exploration techniques uncover geological, geochemical, or geophysical fingerprints for mineralization that have been overlooked in the present interpretation, this area could be prospective.

2. Area 2

Area 2 is located in the center of the survey area and contains all of the mapped prospects or mines other than the Tuscarora mining district. For this reason, Area 2 is ranked as the second priority exploration area. The exploration block can be divided into three subsets; south, central, and north, each containing a fairly distinctive mineralization target.

In the southern one-third of Area 2, the outcropping rock units are similar to those of Area 1, namely ignimbrite (welded-tuff) and andesitic flows. This assemblage possibly indicates the area proximal to a ring fault zone, even though geologic mapping does not show any faults in this area. However, there are two magnetic discontinuities, about one mile apart, that strike east-west through the area. The northernmost of the discontinuities occurs over the contact between the ignimbrite and andesite. The second discontinuity, further south, occurs over rocks mapped as andesitic flows and closely matches the morphology of a major stream valley. It is possible that these east-west striking discontinuities indicate a zone of concentric faults associated with ring faulting. Also, two east-west striking VLF anomalies located in the area between the magnetic discontinuities possibly outline alteration zones. Mineralization targets in this area would be similar to those outlined in the discussion of Area 1 above.

Progressing northward into the middle subset of Area 2, the outcropping rocks here are mapped as ignimbrite containing xenoliths of andesitic rocks. One small outcrop is mapped as rhyolitic to dacitic flows. This area comprises the major anomalously low VLF region. No fewer than three of the mapped prospects occur within positive VLF anomalous zones that surround this low feature. The VLF low is interpreted to be a zone of low conductivity/high resitivity that may be attributed to rocks containing an increased amount of silica. The silica may be associated with silicic alteration or with a compositional variation within the ignimbrite itself, possibly related to a rhyolite dome. The areas that contain the prospects as well as the other VLF zones in the area warrant further exploration.

The northernmost portion of Area 2 contains two magnetic anomalies interpreted to be intrusive rocks at depths of 1500-3000 feet as well as a set of magnetic discontinuities trending north to N30°E. Apparent susceptibilities of these anomalies are over 1000 micro cgs units, similar to the granodioritic rocks of the Mt. Neva pluton to the west. Mapped outcrops consist of ignimbrite. VLF anomalies occur over portions of the interpreted intrusive bodies and may be associated with alteration. Two prospects are located along two different magnetic discontinuities. The targets in this area consist of mineralized hydrothermal systems that might have developed over the interpreted intrusions.

The region immediately to the north of this exploration block contains six interpreted intrusive bodies at depth. They were not included in the exploration block because of the paucity of known mineralization. If mineralization is found to be spatially associated with interpreted intrusives in Area 2, then exploration efforts should also be continued northward to include these interpreted intrusives.

3. Area 3

Area 3 comprises the Mt. Neva granodioritic pluton, and the adjacent siliceous Valmy formation rocks to the south and west, and ignimbrite to the northeast. Only the absence of known mineralization in the immediate vicinity of the pluton reduces the priority of this area. However, the lack of known mineralization does not preclude the possible existence of mineralization. The Divide Mine is located about 2 miles north of Area 3 on the eastern edge of a mapped curvilinear fault that terminates the western end of the pluton. This fault may be a part of a concentric zone of curvilinear faults that make up the western ring fault of the hypothesized caldera. Also, other unnamed, mapped prospects are located less than a mile west of Area 3, just out of the survey area.

Area 3 consists of one large magnetic anomaly that occurs over the mapped granodioritic rocks. This anomaly exhibits apparent susceptibility values of greater than 1000 micro cgs units. From the FVD map, many magnetic discontinuities cut the pluton. Most of the discontinuities are less than one mile in length and trend north-south, with others trending east-west to N25^{o}W. The depths to the top of the magnetic source calculated in this area average over 1000 feet, which indicates the granodioritic porphyry is much more magnetic at depth than at surface. This most likely is related to either oxidation or alteration in the upper portions of the intrusive, or differentiated zones within the instrusive. An anomalous VLF zone nearly completely rings the major portion of the intrusive. This zone consistently contains some of the highest VLF values in the entire Tuscarora survey. The anomalous zone also trends in a N55^{O}E direction from the outcropping pluton toward the other group of interpreted intrusive rocks. This VLF strongly suggests alteration around the pluton.

Mineralization targets in Area 3 consist of metasomatic zones associated with intrusive activity. In the siliceous sediments, zones containing abundant fracturing would be more prospective (for example; the Hilltop Deposit, Lisle and Desrochers, 1988), while in the volcanic rocks, porous and permeable zones exhibiting alteration warrant the highest priority.

4. Area 4

Area 4A occurs in the southern portion of the survey over mapped Tertiary volcanic rocks consisting of ignimbrite. There are no mapped prospects in the area. Area 4A can be broken into two parts, an eastern half and a western half. The eastern half consists of a series of positive magnetic anomalies that occur over ignimbrite. Each of the anomalies has an associated magnetic low, possibly indicative of magnetite depletion and alteration. The western half consists of a series of negative magnetic anomalies over rocks mapped as ignimbrite. This anomalously low area may also be indicative of alteration. Associated with this low is a VLF anomaly which may support the alteration theory. In both halves, magnetic discontinuities trend north-south.

Area 4B occurs in the extreme southeast corner of the survey over the fault bounded contact zone between siliceous sediments and ignimbrite (welded-tuff). The area consists of a negative magnetic anomaly and a VLF anomaly, both of which may represent alteration, and a N25°-35°E magnetic discontinuity. A portion of the VLF anomaly occurs over the major magnetic discontinuity.

VI. CONCLUSIONS AND RECOMMENDATIONS

A. CONCLUSIONS

The aeromagnetic/VLF survey flown over the northern portion of the Tuscarora Mountains yielded the following results.

1. The magnetic results successfully discriminate between the intermediate composition volcanic flows and the two phases of more silicic ignimbrite phase volcanics. The magnetic data also outline areas consisting of granodiorite porphyry (highly magnetic) and siliceous sedimentary rocks (very weakly magnetic).

2. The VLF results appear to outline areas of significant alteration. Positive VLF anomalies are interpreted to be some type of conductive clay alteration, for example propylitic, potassic, or argillic, whereas negative zones are interpreted to represent resistive material and silicic alteration.

3. Magnetic as well as VLF discontinuities appear to indicate geological faults and/or contacts, some of which are related to a postulated ring fault zone associated with a caldera.

4. Four fairly distinct exploration areas have been identified. Exploration areas include: i) the area proximal to the ring fault zone; ii) the area of high-conductivity VLF anomalies surrounding interpreted silicic alteration, iii) the area spacially associated with the granodiorite porphyry intrusive rocks; and iv) the area containing anomalous magnetic and VLF results over fault-bounded volcanic rocks.

B. RECOMMENDATIONS

Although the above described airborne geophysical data provided a wealth of geological information about the survey area, they generally do not provide specific drill targets. Therefore, the following recommendations are provided in an attempt to screen and supplement the airborne data and to provide methods that best delineate mineralization.

1. A thematic-mapper (TM) imagery interpretation of the entire geophysical study area should be undertaken. This study would be very useful for detecting fault patterns associated with possible caldera volcanism such as the ring fault zone, radial faults, or more recent structures that may be associated with mineralization. Also, image processing procedures such as simple band composites, band ratio composites, and principal component composites may be useful for interpreting the extent of alteration zones (Kowalik and Glenn, 1987, Mouat, et al., 1987, and Kepper, et al., 1987).

2. A thorough on-the-ground geologic mapping exercise should be undertaken over each of the four areas recommended for ground follow-up. The objective would be to verify both the alteration zones and discontinuities indicated by the airborne magnetic/VLF data.

3a. A geophysical orientation survey over known mineralized structures in the Tuscarora mining district should be conducted. This survey should include the collection of spectral dipole-dipole induced-polarization/apparent resistivity data and combined magnetic/VLF (OMNI or IGS-2) data.

3b. A geochemical orientation survey over known mineralization in the Tuscarora mining district should also be carried out. This survey should entail the collection of both stream sediment as well as soil samples; with soils being collected either on a grid or using the ridge and spur sampling technique (Rose, and others, 1979). The element analyses required for the orientation should include the following: gold, silver, copper, lead, zinc, arsenic, antimony, mercury, thallium, cadmium, fluorine, bismuth, tellurium, selenium, and tungsten (Berger, 1983). The purpose of this recommendation is to ascertain what sampling methods and element associations best describe an area containing known mineralization.

4. As the above described orientation exercises prove viable exploration techniques, these techniques should be implemented in a systematic exploration program over the four areas recommended for ground follow-up.

VII. REFERENCES

Berger, B.R. 1983, The relationship of alteration and trace-element patterns in epithermal precious-metal-bearing, fossil geothermal systems in the great basin, in The role of heat in the development of energy and mineral resources in the northern Basin and Range province: Geothermal Resources Council, S.R. No. 13, p. 255.

Bonham, H.F., Jr., 1988, Models for volcanic-hosted epithermal precious metal deposits: a review, in Schafer, R.W., Cooper, J.J., and Vikre, P.G., eds., Bulk minable precious metal deposits of the western United States: Geol. Soc. of Nevada, p. 259-272.

Buchanan, L.J., 1981, Precious metal deposits associated with volcanic environments in the southwest, in Dickinson, W.R., and Payne, W.D., eds., Relations of tectonics to ore deposits in the southern Cordillera: Arizona Geol. Soc. Digest, v. 14, p. 237-262.

Coats, R.R., and McKee, E.H., 1972, Ages of plutons and types of mineralization, northwestern Elko County, Nevada: U.S. Geol. Survey Prof. Paper 800-C, p. C165-C168.

Cordell, L. and Grauch, V.J.S., 1982, Reconciliation of the discrete and integral fourier transforms: Geophysics, v.47, No. 2.

Evans, J.G., and Theodore, T.G., 1978, Deformation of the Roberts Mountains allochthon in north-central Nevada: U.S. Geol. Survey Prof. Paper 1060, 18 p.

Granger, A.E., Bell, M.M., Simmons, G.C., Lee, F., 1957, Geology and mineral resources of Elko County, Nevada: Nevada Bur. Mines, Bull. 54, 190 p.

Guilbert, J.M. and Park, C.F., 1986, The geology of ore deposits: W.H.Freeman and Company, New York.

Gunn, P.J., 1975, Linear transformation of gravity and magnetic fields: Geophysical Prospecting v.23, p.300-312.

Hood, P.J., Holroyd, M.T. and McGrath, P.H., 1979, Magnetic methods applied to base metal exploration, in Geophysics and geochemistry in the search for metallic ores: Geol. Survey of Canada, Economic Geology Report 31.

Kepper, J.C., Lugaski, T.P., and MacDonald, J.S., 1987, Discrimination of lithologic units, alteration patterns and major structural blocks in the Tonapah, Nevada area using thematic mapper data, in Proceedings of the fifth thematic conference on remote sensing for exploration geology, mineral and energy exploration: technology for a competitive world: Environmental Research Institute of Michigan, p. 97-115.

Ketner, K.B., 1977, Late Paleozoic orogeny and sedimentation, southern California, Nevada, Idaho, and Montana, in Stewart, J.H., Stevens, C.H., and Fritsche, A.E., eds., Paleozoic paleogeography of the western United States: Soc. Econ. Paleontologists and Mineralogists, Pacific Section, Pacific Coast Paleogeography Symposium 1, p. 363-369.

Kowalik, W.S., and Glenn, W.E., 1987, Image processing of aeromagnetic data and integration with Landsat images for improved structural interpretation: Geophysics, v. 52, no. 7, p. 875-884.

Lipman, P.W., 1981, The Miocene Questa caldera, northern New Mexico: relation to batholith emplacement and associated molybdenum mineralization, in The genesis of Rocky Mountain ore deposits; changes with time and tectonics: Denver Region Exploration Geologist Society, p. 133-150.

____________, 1982, Volcano-tectonic setting of Tertiary ore deposits, southern Rocky Mountains, in Dickinson, W.R., and Payne, W.D., eds., Relations of tectonics to ore deposits in the southern Cordillera: Arizona Geol. Soc. Digest, v.14, p. 199-214.

____________, 1984, The roots of ash flow calderas in western North America: windows into the tops of granitic batholiths J. Geophys. Res., v. 89, No. B10, p. 8801-8841.

Lisle, R.E., and Desrochers, G.J., 1988, Geology of the Hilltop gold deposit, Lander County, Nevada, in Schafer, R.W., Cooper, J.J., and Vikre, P.G., eds., Bulk minable precious metal deposits of the western United States: Geol. Soc. of Nevada, p. 101-118.

McKee, E.H., and Coats, R.R., 1975, K-Ar age of ore deposition, Tuscarora mining district, Elko County, Nevada: Isochron/West, no. 13, p. 11-12.

Mouat, D.A., Myers, J.S., and Miller, N.L., 1987, An integrated approach to the use of Landsat TM data for gold exploration in west central Nevada: in Proceedings of the fifth thematic conference on remote sensing for exploration geology, mineral and energy exploration: technology for a competitive world: Environmental Research Institute of Michigan, p. 615-626.

Nolan, T.B., 1936, The Tuscarora mining district, Nevada: Nevada Univ. Bull., V. 30, 38 p.

Phillips, W.J., and Richards, W.T., 1975, A study of the effectiveness of the VLF method for the location of narrow, mineralized fault zones: Geo-exploration, 13, p. 215-226.

Roberts, R.J., 1964, Stratigraphy and structure of the Antler Peak quadrangle, Humboldt and Lander Counties, Nevada: U.S. Geol. Survey Prof. Paper 459-A, 93 p.

Roberts, R.J., Radtke, A.S., and Coats, R.R., 1971, Gold bearing deposits in north-central nevada and southwestern Idaho: Econ. Geol., v. 66, p. 14-33.

Rose, A.W., Hawkes, H.E., and Webb, J.S., 1979, Geochemistry in mineral exploration: Academic Press, London, 657 p.

Rytuba, J.J., 1981, Relation of calderas to ore deposits in the western United States, in Dickinson, W.R., and Payne, W.D., eds., Relations of tectonics to ore deposits in the southern Cordillera: Arizona Geol. Soc. Digest, v. 14, p. 227-236.

Sibbett, B.S., 1982, Geology of the Tuscarora geothermal prospect, Elko County, Nevada: Geol. Soc. American Bull., v. 93, p. 1264-1272.

Silberling, N.J. and Roberts, R.J., 1962, Pre-Tertiary stratigraphy and structure of northwestern Nevada: Geol. Soc. America Spec. Paper 72, 58 p.

Silberman, M.L., 1983, Geochronology of hydrothermal alteration and mineralization: Tertiary epithermal precious metal deposits in the Great Basin, in The role of heat in the development of energy and mineral resources in the northern Basin and Range province: Geothermal Resources Council, S.R. No. 13, p. 287-303.

Smith, J.G., McKee, E.H., Tatlock, D.B., Marvin, R.F., 1971, Mesozoic granitic rocks in northwestern Nevada: a link between the Sierra Nevada and Idaho batholiths: Geol. Soc. America Bull., v. 83, p. 2933-2944.

Smith, J.F., Jr., and Ketner, K.B., 1968, Devonian and Mississippian rocks and the date of the Roberts Mountains thrust in the Carlin-Pinon Range area, Nevada: U.S. Geol. Survey Bull. 1251-I, p. I1-I18.

Spector, A., 1968, Spectral analysis of aeromagnetic data: Unpub. Ph.D. Thesis, Dept. of Physics, University of Toronto.

Spector, A., 1975, Applications of aeromagnetic data for porphyry copper exploration in areas of volcanic cover, Reprint of paper delivered at the 45th Annual International Meeting of the Society of Exploration Geophysicists, October 15, 1975, Denver, Colorado.

Spector, A. and Grant, F.S., 1970, Statistical model for interpretation of aeromagnetic data: Geophysics, v.35, no. 2.

Speed, R.C., 1983, Precenozoic tectonic evolution of northeastern Nevada, in The role of heat in the development of energy and mineral resources in the northern Basin and Range province: Geothermal Resources Council, S.R. No. 13, p. 11-24.

Stewart, J.H., 1980, Geology of Nevada: Nevada Bur. Mines Special Publication 4, 136 p.

______________, 1983, Cenozoic structure and tectonics of the northern Basin and Range, province, California, Nevada, and Utah, in The role of heat in the development of energy and mineral resources in the northern Basin and Range province: Geothermal Resources Council, S.R. No. 13, p. 25-40.

Stewart, J. H., and Carlson, J.E., 1976, Cenozoic rocks of Nevada: Nevada Bur. Mines and Geol., Map 52.

Willden, R., 1961, Preliminary geologic map of Humboldt County Nevada: U.S. Geol. Survey Mineral Inv. Field Studies Map MF-236, 1:200,000.

Worthington, J.E., 1982, Bulk tonnage gold deposits in volcanic environments, in Dickinson, W.R., and Payne, W.D., eds., Relations of tectonics to ore deposits in the southern Cordillera: Arizona Geol. Soc. Digest, v. 14, p. 263-270.

Yarger, H.L., Robertson, R.R., and Wentland, R.L., 1978, Diurnal drift removal from aeromagnetic data using least squares: Geophysics, p.1148-1156.

Yunsheng, S., Strangway, D.W. and Urquhart, W.E.S., 1985, Geological interpretation of a high-resolution aeromagnetic survey in the Amos-Barraute area of Quebec, in The utility of regional gravity and magnetic anomaly maps: Hinze, W.J., ed. Society of Exploration Geophysicists.

APPENDIX A

SURVEY FLIGHT LINE INFORMATION

SURVEY FLIGHT LINE INFORMATION

Aeromagnetic / VLF survey
Tuscarora Range, Nevada
Chevron

LINE NUMBER	FLIGHT NUMBER	DATE JD YR	FIRST FIDUCIAL	LAST FIDUCIAL	HEADING (deg)	LENGTH (km)
10	2	14 1989	143479	144246	180.	16.7
20	2	14 1989	141315	142084	180.	16.6
30	2	14 1989	139204	139894	180.	15.9
40	2	14 1989	137183	137873	180.	15.7
50	2	14 1989	135262	135923	180.	15.1
60	2	14 1989	133376	134042	180.	14.8
70	2	14 1989	142484	143230	0.	15.6
80	2	14 1989	140288	141056	0.	15.6
91	2	14 1989	144536	145370	0.	16.1
100	2	14 1989	136190	136960	0.	16.1
110	2	14 1989	134262	135014	0.	15.8
120	2	14 1989	132348	133080	0.	15.8
130	2	14 1989	131144	131862	180.	15.7
140	1	13 1989	123007	124376	180.	25.8
150	1	13 1989	119734	121148	180.	25.0
160	1	13 1989	116400	117821	180.	26.7
170	1	13 1989	126234	127676	180.	26.6
180	1	13 1989	129313	130664	180.	25.1
190	1	13 1989	132412	133805	180.	25.1
200	2	14 1989	120270	121468	180.	26.3
210	2	14 1989	124954	126159	180.	26.1
220	2	14 1989	128028	129212	180.	25.7
230	1	13 1989	118259	119327	0.	24.0
240	1	13 1989	121548	122638	0.	23.9
250	1	13 1989	124774	125790	0.	23.6

SURVEY FLIGHT LINE INFORMATION

Aeromagnetic / VLF survey
Tuscarora Range, Nevada
Chevron

LINE NUMBER	FLIGHT NUMBER	DATE JD	DATE YR	FIRST FIDUCIAL	LAST FIDUCIAL	HEADING (deg)	LENGTH (km)
260	1	13	1989	127932	129050	0.	26.2
270	1	13	1989	130950	132070	0.	26.5
280	2	14	1989	118676	119910	0.	26.4
290	2	14	1989	123365	124636	0.	27.1
300	2	14	1989	126423	127613	0.	25.4
310	2	14	1989	129470	130694	0.	26.6
320	2	14	1989	145896	147088	180.	25.7
330	2	14	1989	150422	151703	180.	26.1
340	2	14	1989	154529	155829	180.	26.8
352	6	18	1989	113645	114719	0.	25.7
360	2	14	1989	157708	159188	180.	29.8
370	2	14	1989	161000	162452	180.	29.3
381	6	18	1989	115224	116520	180.	29.6
391	6	18	1989	118323	119594	180.	29.3
400	6	18	1989	121410	122655	180.	29.1
410	6	18	1989	125280	126518	180.	28.6
420	6	18	1989	128330	129585	180.	29.0
430	6	18	1989	131380	132673	180.	29.1
440	2	14	1989	152780	154127	0.	29.9
450	2	14	1989	156085	157442	0.	30.1
460	2	14	1989	159422	160796	0.	30.4
472	6	18	1989	116772	117996	0.	29.2
481	6	18	1989	119892	121099	0.	29.1
490	6	18	1989	123732	124970	0.	29.7
500	6	18	1989	126834	128025	0.	28.6

SURVEY FLIGHT LINE INFORMATION

Aeromagnetic / VLF survey
Tuscarora Range, Nevada
Chevron

LINE NUMBER	FLIGHT NUMBER	DATE JD	YR	FIRST FIDUCIAL	LAST FIDUCIAL	HEADING (deg)	LENGTH (km)
510	6	18	1989	129864	131092	0.	28.5
520	6	18	1989	133001	134292	0.	29.8
530	6	18	1989	136425	137687	0.	28.6
540	6	18	1989	140076	141321	0.	28.5
550	6	18	1989	143433	144650	0.	28.3
560	6	18	1989	150790	152120	0.	29.8
570	6	18	1989	153943	155203	0.	28.6
580	6	18	1989	157038	158329	0.	28.5
590	6	18	1989	160161	161505	0.	28.8
600	6	18	1989	161800	163120	0.	29.0
610	6	18	1989	134745	136028	180.	28.7
621	6	18	1989	138090	139430	180.	28.8
631	6	18	1989	141702	142970	180.	28.4
644	6	18	1989	152387	153657	180.	28.4
651	6	18	1989	155450	156741	180.	29.0
661	6	18	1989	158583	159850	180.	28.0
671	8	20	1989	123762	125051	0.	28.7
681	8	20	1989	121820	123265	180.	29.1
690	4	17	1989	174813	176131	180.	29.9
692	8	20	1989	118547	119943	180.	29.2
700	7	18	1989	222768	224070	180.	29.3
710	7	18	1989	219836	221073	180.	28.1
720	7	18	1989	216647	217902	180.	28.4
730	7	18	1989	213584	214860	180.	29.0
741	7	18	1989	210543	211820	180.	29.0

SURVEY FLIGHT LINE INFORMATION

Aeromagnetic / VLF survey
Tuscarora Range, Nevada
Chevron

LINE NUMBER	FLIGHT NUMBER	DATE JD	DATE YR	FIRST FIDUCIAL	LAST FIDUCIAL	HEADING (deg)	LENGTH (km)
751	8	20	1989	120284	121530	0.	29.9
760	5	17	1989	207297	208566	0.	29.8
761	8	20	1989	116975	118218	0.	30.1
771	7	18	1989	224290	225519	0.	29.8
781	7	18	1989	221290	222488	0.	29.3
791	7	18	1989	218345	219549	0.	28.7
801	7	18	1989	215130	216347	0.	28.8
811	7	18	1989	212093	213322	0.	29.4
821	7	18	1989	205062	205830	0.	17.7
831	7	18	1989	209448	210238	0.	18.3
841	7	18	1989	208235	209061	0.	18.3
851	7	18	1989	207191	207990	0.	18.7
861	7	18	1989	206040	206864	0.	18.5
871	7	18	1989	203875	204720	0.	18.7
881	7	18	1989	201770	202570	0.	17.9
890	3	14	1989	233482	234252	180.	16.8
900	3	14	1989	231368	232098	180.	15.9
911	1	13	1989	137925	138859	180.	17.6
920	1	13	1989	140510	141400	180.	16.6
931	7	18	1989	199857	200530	180.	15.0
941	7	18	1989	198030	198683	180.	14.5
951	7	18	1989	196107	196840	180.	16.5
961	7	18	1989	191622	192353	180.	15.8
971	7	18	1989	193630	194350	180.	16.2
981	7	18	1989	202860	203550	0.	16.2

SURVEY FLIGHT LINE INFORMATION

Aeromagnetic / VLF survey
Tuscarora Range, Nevada
Chevron

LINE NUMBER	FLIGHT NUMBER	DATE JD	YR	FIRST FIDUCIAL	LAST FIDUCIAL	HEADING (deg)	LENGTH (km)
991	7	18	1989	200807	201496	0.	16.1
1001	7	18	1989	198930	199600	0.	15.7
1011	7	18	1989	197074	197768	0.	16.1
1021	7	18	1989	194797	195434	0.	15.2
1031	7	18	1989	192610	193316	0.	16.3
1041	7	18	1989	190291	190982	0.	16.1
1050	3	14	1989	232448	233145	0.	16.2
1060	1	13	1989	139323	140080	0.	16.2
1070	1	13	1989	135830	136553	0.	16.2
1110	3	14	1989	218666	219454	270.	17.7
1120	3	14	1989	219844	220608	90.	17.7
1130	3	14	1989	216403	217202	270.	17.2
1140	3	14	1989	217544	218294	90.	18.0
1150	3	14	1989	215160	215932	90.	19.2
1160	3	14	1989	213849	214755	270.	18.8
1170	3	14	1989	212534	213588	90.	24.2
1180	3	14	1989	210835	212090	270.	24.4
1190	3	14	1989	203370	204358	90.	23.9
1200	3	14	1989	206356	207405	90.	24.5
1210	3	14	1989	209311	210316	90.	24.1
1220	3	14	1989	201886	203000	270.	23.6
1230	3	14	1989	204750	205938	270.	23.6
1240	3	14	1989	207766	208946	270.	24.0
1250	3	14	1989	221332	222407	270.	22.8
1260	3	14	1989	224042	225084	270.	22.6

SURVEY FLIGHT LINE INFORMATION

Aeromagnetic / VLF survey
Tuscarora Range, Nevada
Chevron

LINE NUMBER	FLIGHT NUMBER	DATE JD YR	FIRST FIDUCIAL	LAST FIDUCIAL	HEADING (deg)	LENGTH (km)
1270	3	14 1989	225438	226437	90.	23.6
1280	3	14 1989	200380	201376	90.	23.3
1290	3	14 1989	222742	223620	90.	20.5
1301	3	14 1989	227946	228774	270.	17.1
1310	3	14 1989	229306	230162	90.	19.9
1320	3	14 1989	199126	200028	270.	19.0
1330	3	14 1989	196765	197634	270.	18.0
1340	3	14 1989	198001	198800	90.	18.1
1350	3	14 1989	194524	195296	270.	16.5
1360	3	14 1989	195717	196360	90.	15.2
1371	8	20 1989	127022	127731	90.	14.9
1380	3	14 1989	192280	193072	270.	17.5
1391	8	20 1989	129330	130093	90.	15.6
1400	3	14 1989	185607	186440	270.	17.0
1410	3	14 1989	187890	188686	270.	16.6
1421	8	20 1989	128210	128973	270.	15.7
1430	3	14 1989	188966	189679	90.	16.3
1441	3	14 1989	186832	187534	90.	15.8

Ward:

4950 0047

HIGH SENSITIVITY AEROMAGNETIC

AND VLF ELECTROMAGNETIC SURVEY

NORTHERN TUSCARORA MOUNTAINS, NEVADA

Prepared For:

CHEVRON RESOURCES COMPANY

4000 EXECUTIVE PARKWAY

P. O. BOX 5049

SAN RAMON, CALIFORNIA 94583-0949

Copy 1 – RENO (of 2)

Prepared By:

BARRINGER GEOSERVICES, INC.

15000 WEST 6TH AVENUE

SUITE 300

GOLDEN, COLORADO 80401

MAY, 1989

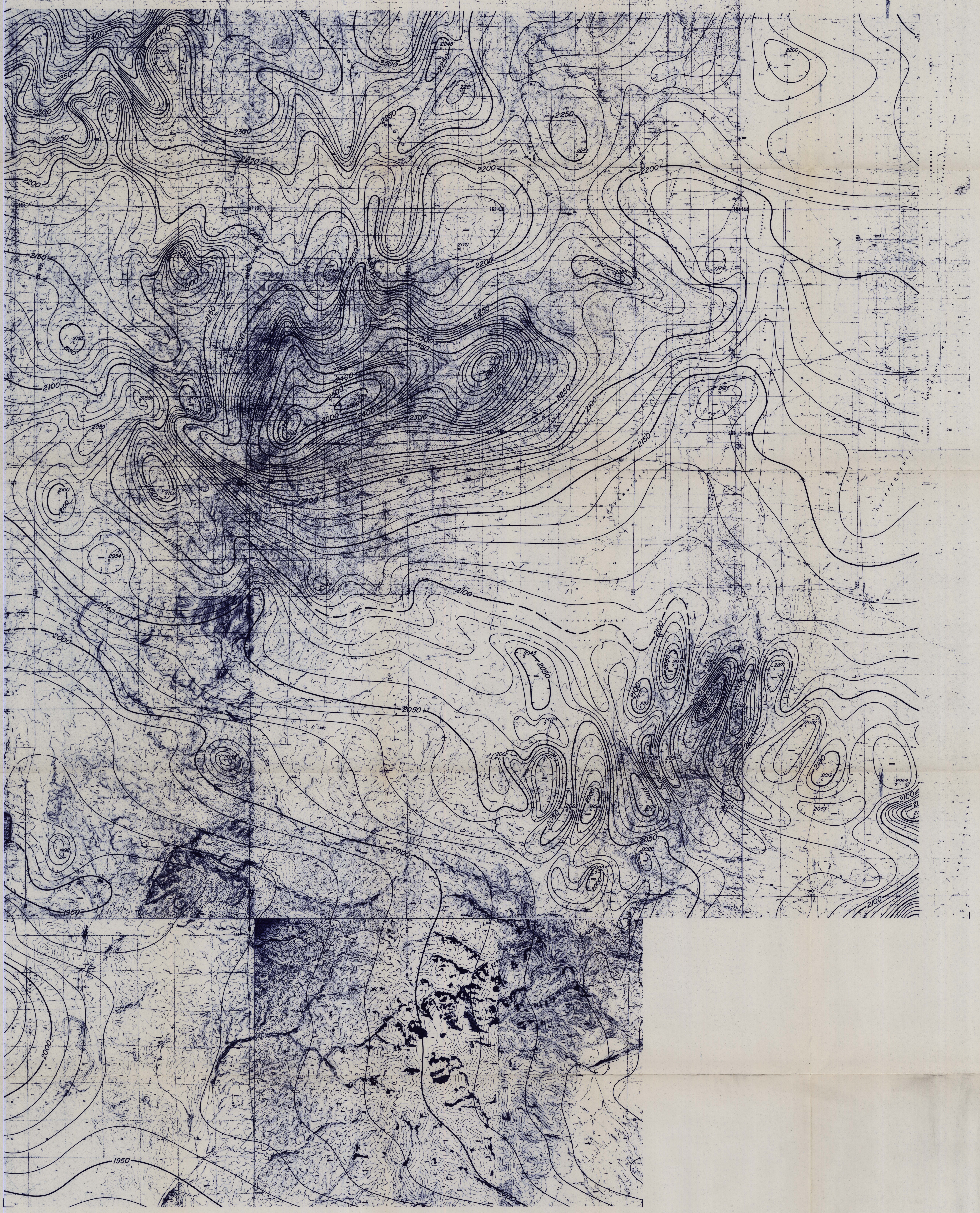

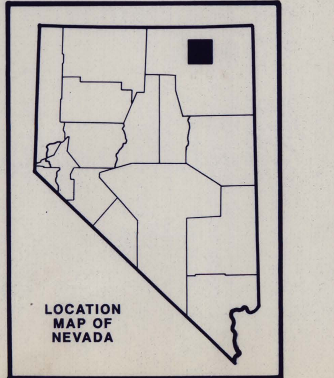

4000 0 4000
SCALE IN FEET

4950 0047

Revisions

Overlays

Chevron

Chevron Resources Company
Domestic Minerals Exploration Division

TUSCARORA
Elko Co., Nevada

U.S.G.S.
REGIONAL AEROMAGNETIC MAP

SCALE	DATE	Author:	Map No. MD-8073-ME
1"= 4000'	8/2/90	Dwn. By: Ck. By:	Tube No. 700

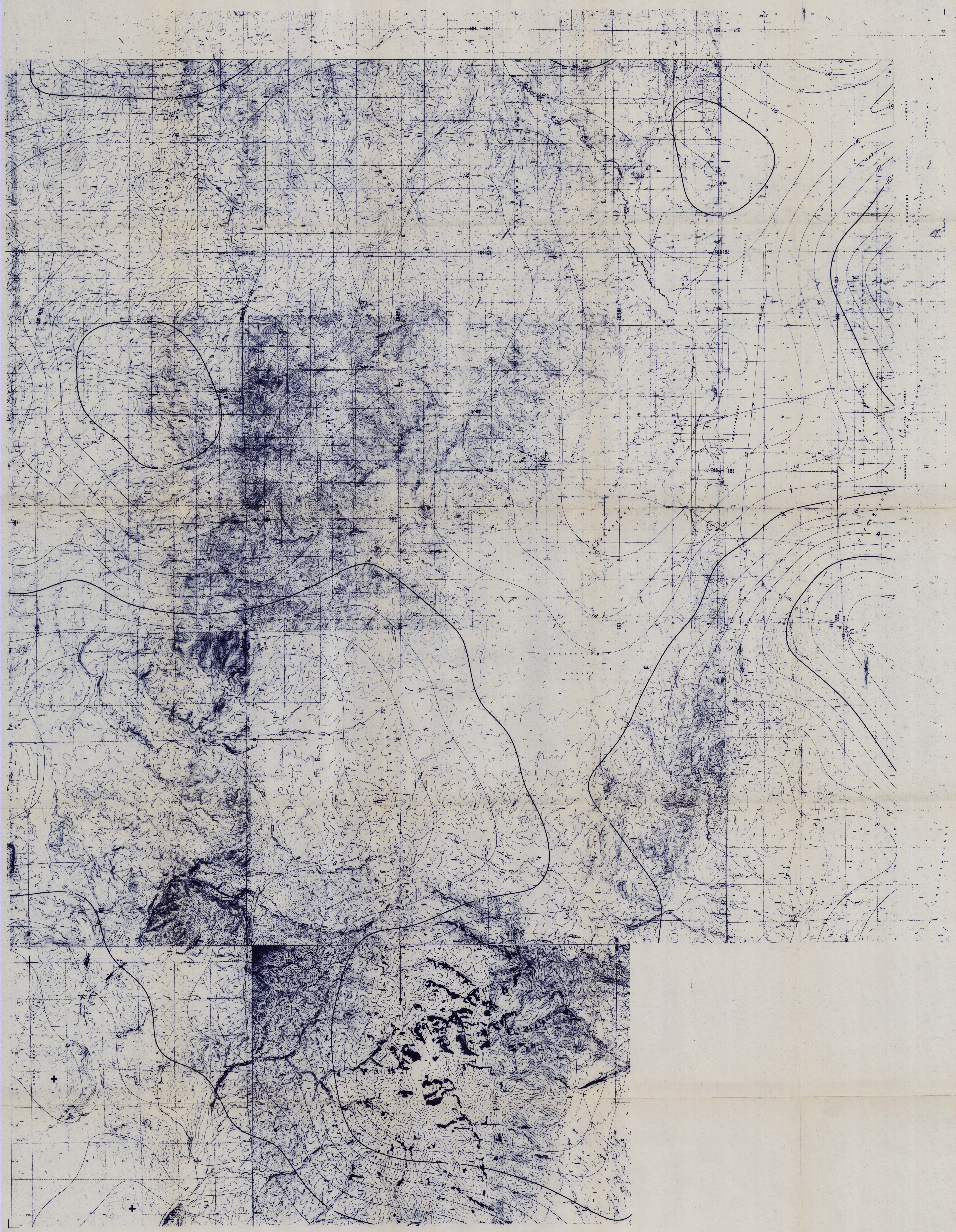

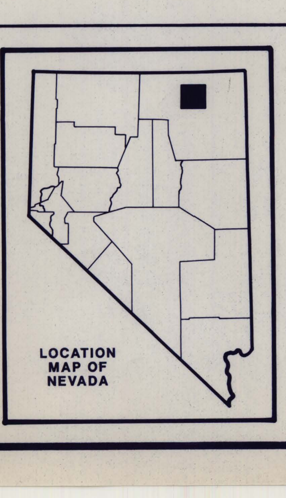

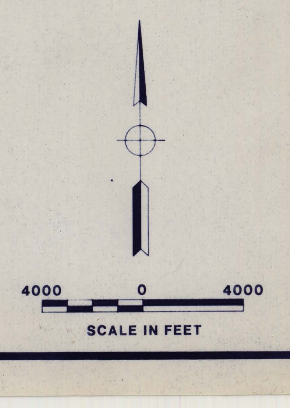

4950 0047

Chevron

Chevron Resources Company
Domestic Minerals Exploration Division

TUSCARORA

Elko Co., Nevada

U.S.G.S. REGIONAL GRAVITY RESIDUAL MAP

Revisions

Overlays

SCALE	DATE	Author: Dwn. By: Ck. By:	Map No. MD-8073-ME
1"= 4000'	8/2/90		Tube No. 700

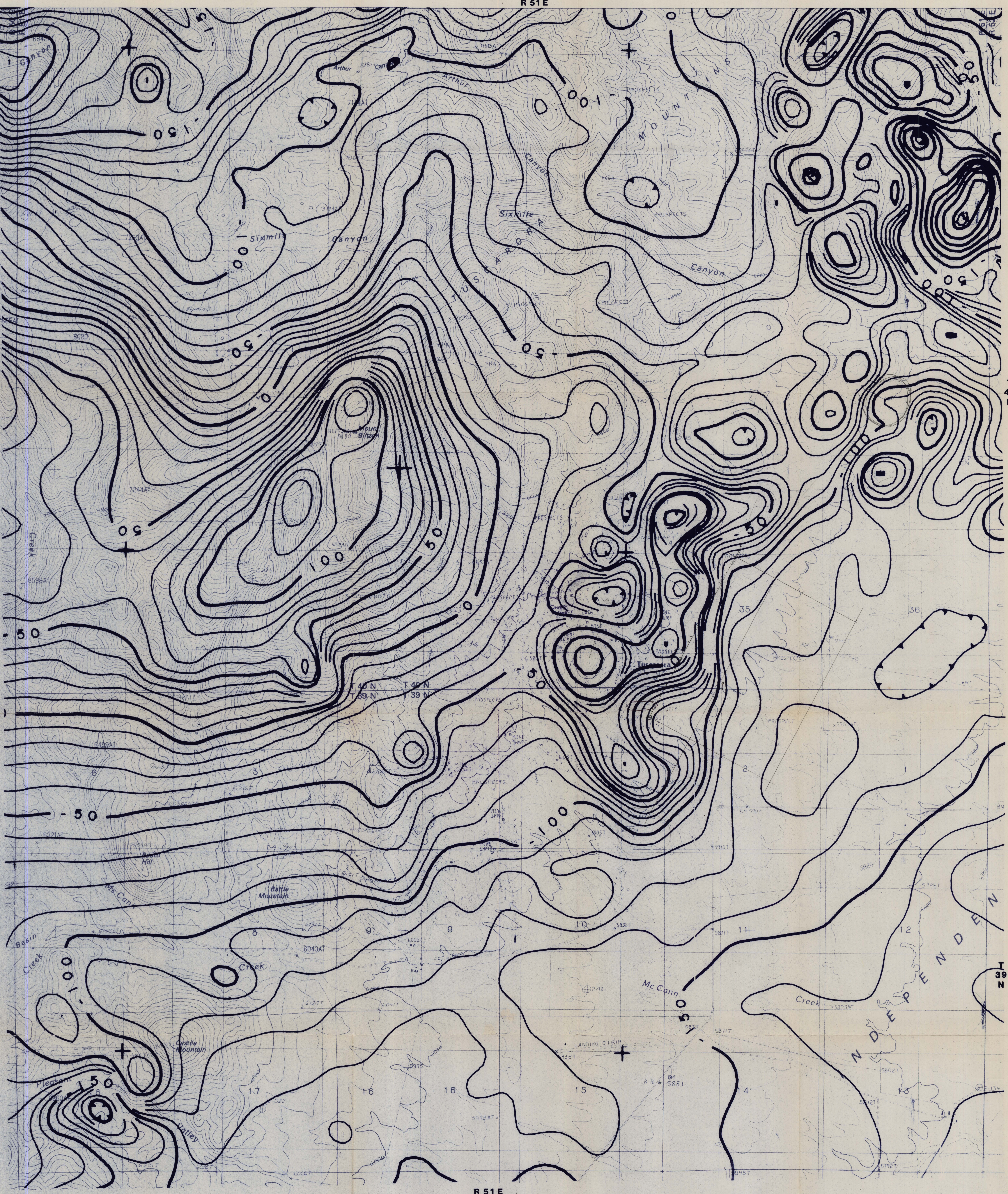

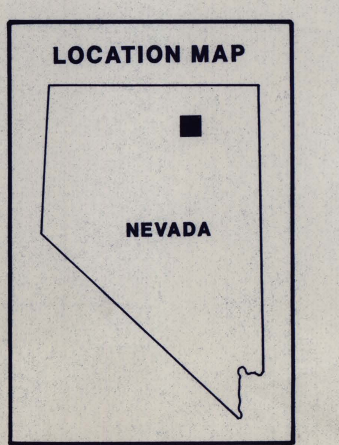

SCALE IN FEET

4950 0047

Revisions	Chevron Resources Company Domestic Minerals Exploration Division		
	TUSCARORA Elko Co., Nevada Airborne Total Magnetic Intensity (Barringer)		
Overlays	SCALE: 1"= 1000'	DATE: 4/26/90	Author: Dwn. By: Ck. By:
	Map No. MD-8066-ME	Tube No. 700	

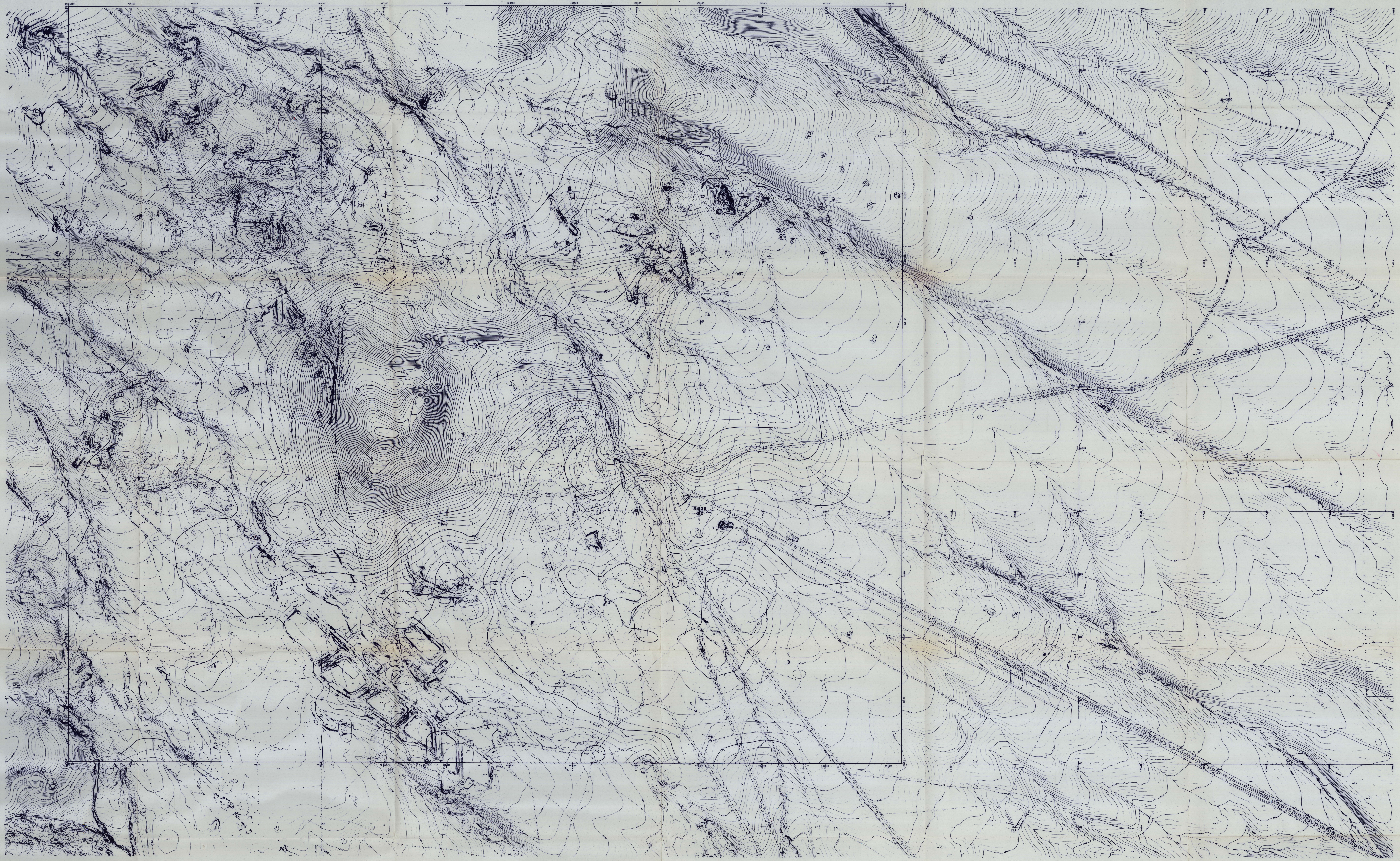

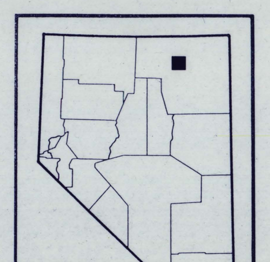

LOCATION MAP OF NEVADA

200 0 200
SCALE IN FEET

Revisions	Chevron Resources Company Domestic Minerals Exploration Division		
	TUSCARORA **Central District** **Elko Co., Nevada** **GROUND MAG**		
Overlays	DATA: Fischer-Watt, Tuscarora Project, Magnetic Map 4/21/84.		
	SCALE 1"=200'	DATE 5/16/90	Author: Dwn. By: B. EASTERLY Ck. By:
	Map No. MD-8081-ME Tube No. 702		

4950 0047

4950 0047